REVIEWS

Journal of Semiconductors
(2022) 43, 041106
doi: 10.1088/1674-4926/43/4/041106

Recent progress on advanced transmission electron microscopy characterization for halide perovskite semiconductors

Xiaomei Wu, Xiaoxing Ke†, and Manling Sui†

Faculty of Materials and Manufacturing, Beijing University of Technology, Beijing 100124, China

Abstract: Halide perovskites are strategically important in the field of energy materials. Along with the rapid development of the materials and related devices, there is an urgent need to understand the structure–property relationship from nanoscale to atomic scale. Much effort has been made in the past few years to overcome the difficulty of imaging limited by electron dose, and to further extend the investigation towards operando conditions. This review is dedicated to recent studies of advanced transmission electron microscopy (TEM) characterizations for halide perovskites. The irradiation damage caused by the interaction of electron beams and perovskites under conventional imaging conditions are first summarized and discussed. Low-dose TEM is then discussed, including electron diffraction and emerging techniques for high-resolution TEM (HRTEM) imaging. Atomic-resolution imaging, defects identification and chemical mapping on halide perovskites are reviewed. Cryo-TEM for halide perovskites is discussed, since it can readily suppress irradiation damage and has been rapidly developed in the past few years. Finally, the applications of *in-situ* TEM in the degradation study of perovskites under environmental conditions such as heating, biasing, light illumination and humidity are reviewed. More applications of emerging TEM characterizations are foreseen in the coming future, unveiling the structural origin of halide perovskite's unique properties and degradation mechanism under operando conditions, so to assist the design of a more efficient and robust energy material.

Key words: organic–inorganic hybrid perovskite solar cell materials; energy materials; scanning electron microscopy; transmission electron microscopy; irradiation damage

Citation: X M Wu, X X Ke, and M L Sui, Recent progress on advanced transmission electron microscopy characterization for halide perovskite semiconductors[J]. *J. Semicond.*, 2022, 43(4), 041106. https://doi.org/10.1088/1674-4926/43/4/041106

1. Introduction

The fast rising of halide perovskites has drawn significant attention in the field of energy materials in the past decade. Owning to their unique structure, high degree of tunability, and excellent photoelectric properties, halide perovskites have been widely used in photovoltaic and optoelectronic devices, including solar cells, LED, and photodetectors[1–5]. Taking $CH_3NH_3PbI_3$ (referred as $MAPbI_3$) as an example, it is a prototypical organic–inorganic hybrid perovskite used in emerging photovoltaic material, and has a bandgap of about 1.55 eV, large absorption coefficient similar to Si, better tolerance to defect, high carrier mobility, long length of electron–hole transport and thus high conversion efficiency[6, 7]. In addition, it can be prepared as thin films for flexible devices, easy to synthesize and allows scaling-up for production[8, 9]. In just a few years, the conversion efficiency of the perovskite solar cell (PSC) using $MAPbI_3$ as the light-absorption layer has increased from 3.8% to 25.7% as reported in a most recently published paper[10]. By replacing the A-site cation with other organic moieties and doping at the B-site/X-site, not only the bandgap can be tuned, but also its stability under environmental conditions can be improved, thereby providing more possibilities for the developments and applications of halide perovskites[11–13]. In addition, two-dimensional (2D) nanosheets, one-dimensional (1D) nanowires[14, 15], all-inorganic quantum dots such as $CsPbX_3$[16, 17], Pb-free double perovskites nanostructures[18–23] have also demonstrated remarkable performance and unlimited applications for light-emitting devices and photodetectors etc.

The unusual optoelectronic properties and performance of halide perovskites are closely related to their unique crystal structure and microstructure. The name of the perovskite is originated from the calcium titanate ($CaTiO_3$) compound in the perovskite mineral, and is referred to as ABX_3 compound (where A and B are cations and X is an anion). In perovskite structure, $[BX_6]$ octahedra are corner-sharing to be ordered in a cubically, where the cations at A-site are located in the center of cubic cage[24]. Halide perovskites have similar structures following the general form of ABX_3, where the A site is a monovalent cation, such as $CH_3NH_3^+$ (R_A = 0.18 nm), $CH_3CH_2NH_3^+$ (R_A = 0.23 nm), $NH_2CH{=}NH_2^+$ (R_A ≈ 0.19–0.22 nm), or inorganic cations such as Cs^+ (R_A = 0.167 nm), Rb^+ (R_A = 0.152 nm), K^+ (R_A = 0.138 nm); the B site is mostly divalent cations such as Pb^{2+} (R_B = 0.119 nm), Sn^{2+} (R_B = 0.112 nm); the X site is a halogen anion such as Cl^- (R_X = 0.181 nm), Br^- (R_X = 0.196 nm), I^- (R_X = 0.220 nm). Additionally, when the B site Pb^{2+} ion is replaced by a monovalent cation and a trivalent cation, an inorganic Pb-free double perovskite is formed, written as $A_2BB'X_6$, such as $Cs_2AgInCl_6$, $Cs_2AgBiBr_6$ and $Cs_2AgBiCl_6$. The unique perovskite structure, e.g. the crystal symmetry, the vibration and ordered arrangement of the organic groups, and the tilt of the $[PbI_6]$ octahedra have shown to be related to their photovoltaic proper-

Correspondence to: X X Ke, kexiaoxing@bjut.edu.cn; M L Sui, mlsui@bjut.edu.cn

Received 28 FEBRUARY 2022; Revised 25 MARCH 2022.

ties[25]. For all-inorganic halide perovskite such as $CsPbX_3$, it is known to own multiple phases and is therefore possible to form nano-domain structure at the coexistence of multi-phases, which further influences its photoelectric properties[26]. Chemical composition inhomogeneity, strain distribution, polarization, defects such as domain walls, grain boundaries and surface defects are also known to influence the materials' properties and performances[27–30]. It is hence of great importance to study the microstructures and their degradation under operando conditions and to understand the relationship between properties and microstructures[31–33].

Transmission electron microscopy (TEM) is one of the most straightforward characterization techniques to investigate the microstructure from nanometer to the atomic scale[34–37]. Along with the rapid developments of halide perovskites, much progress has been achieved in the past few years. Rothmann *et al.* were one of the first research groups to report twinning structure in the as-grown $MAPbI_3$ single crystal sample using electron diffraction[38]. The atomic-resolution structure of $MAPbI_3$ was further revealed using direct electron detector and cryo-TEM, respectively[39, 40]. Yu *et al.* reported a nanodomain structure in $CsPbBr_3$ 2D nanocrystals where tetragonal and cubic phases coexist[41]. On the other hand, *in-situ* TEM and quasi-*in-situ* TEM has been developed on cross-sectional samples from $MAPbI_3$ PSCs, where ion migration and degradation of the perovskite thin film under environmental conditions have been studied in nanoscale[42–44]. However, the microstructural investigation of halide perovskites using TEM has been significantly constrained by its extreme sensitivity to electron beams. The inevitable knock-on damage and radiolysis damage on halide perovskites accelerate its degradation in TEM, complicating the interpretation of as-observed phenomena: when irradiated by electron beams, the halogen ions rapidly desorb from the structure and the organic moieties easily break down due to radiolysis, resulting in structure collapse[3, 45]. As reported by Rothmann *et al.* and confirmed by other TEM study, a total dose of <100 e/Å^2 can destruct halide perovskite[46], which is far below the imaging condition for conventional TEM study.

Driven by the urgent need to understand the microstructure–properties relationship for halide perovskites which is strategically important, much effort has been made in the past few years to overcome the difficulty of imaging limited by electron dose, and to further extend the investigation towards operando conditions. This review is therefore dedicated to recent studies of advanced TEM characterizations for halide perovskites. Firstly, the irradiation damage and "artefacts" caused by the interaction of electron beams and perovskites under conventional imaging conditions are summarized and discussed, calling attention to the interpretation of TEM results for this particular materials. Low-dose TEM is then discussed, including conventional technique of electron diffraction and emerging techniques for high-resolution TEM (HRTEM) imaging. Atomic-resolution imaging and defects identification on halide perovskites are reviewed. Composition analysis using energy dispersive X-ray microscopy (EDX) and electron energy loss spectroscopy (EELS) mapping are also discussed. Cryo-TEM for halide perovskites is then given special attention in this review, since it can readily suppress irradiation damage and has been rapidly developed for imaging beam-sensitive energy materials in the past few years. Finally, the applications of *in-situ* TEM in the degradation study of perovskites under environmental conditions such as heating, biasing, light illumination and humidity are reviewed. An illustration of advanced TEM characterizations for halide perovskites is presented in Fig. 1.

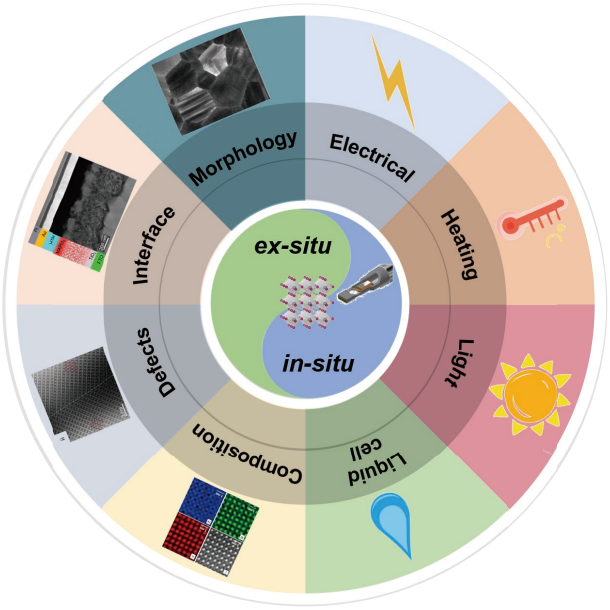

Fig. 1. (Color online) Schematic illustration of advanced TEM characterization for halide perovskites.

2. Irradiation damage on halide perovskites by conventional TEM imaging

The irradiation damage induced by energetic electrons during the imaging of halide perovskites has significantly limited the TEM characterization, and is considered as the cornerstone for the interpretation of as-observed microstructures.

When organic–inorganic hybrid perovskites are imaged using conventional TEM, the structure of the halide perovskites can be destroyed in seconds, resulting in the irradiation damage such as generation of "bubbles" and precipitation of nanoparticles, as shown in Fig. 2. Chen *et al.* noticed severe damage in the $MAPbI_3$ perovskite polycrystalline film when imaged at a relatively high electron dose of ~9870 e/(Å^2·s) (i.e. the dose for obtaining conventional HRTEM images), where nanoparticles precipitated quickly within the irradiated area (Fig. 2(a)). Such irradiation damage was attributed to the electric field generated by the electron beam within the perovskite, and remained by reducing electron dose to 500 e/(Å^2·s)[47, 48]. On the other hand, Kim *et al.* revealed the generation and expansion of "bubbles" by obtaining a series of TEM images through continuous irradiation on $MAPbI_3$ perovskite single crystals (Fig. 2(b))[49]. In general, the degradation of organic–inorganic hybrid halide perovskites in vacuum or in air has been frequently noticed, and the precipitated nanofragmentaions are mostly identified mostly as PbI_2 or Pb clustering[50, 51]. In addition, 2D organic-inorganic hybrid halide perovskites are more susceptible to electron beam damage due to the presence of interlayer organic ligands, and very few TEM studies on 2D perovskites were reported. Dou *et al.* attempted to study $(C_4H_9NH_3)_2PbBr_4$ (i.e. BA_2PbBr_4) by TEM, which degraded rapidly into Pb nanoparticles under a very low dose[52]. Nie *et al.* reported the same phenomenon in the study of BA_2PbBr_4 nanosheets, where the nanoparticles

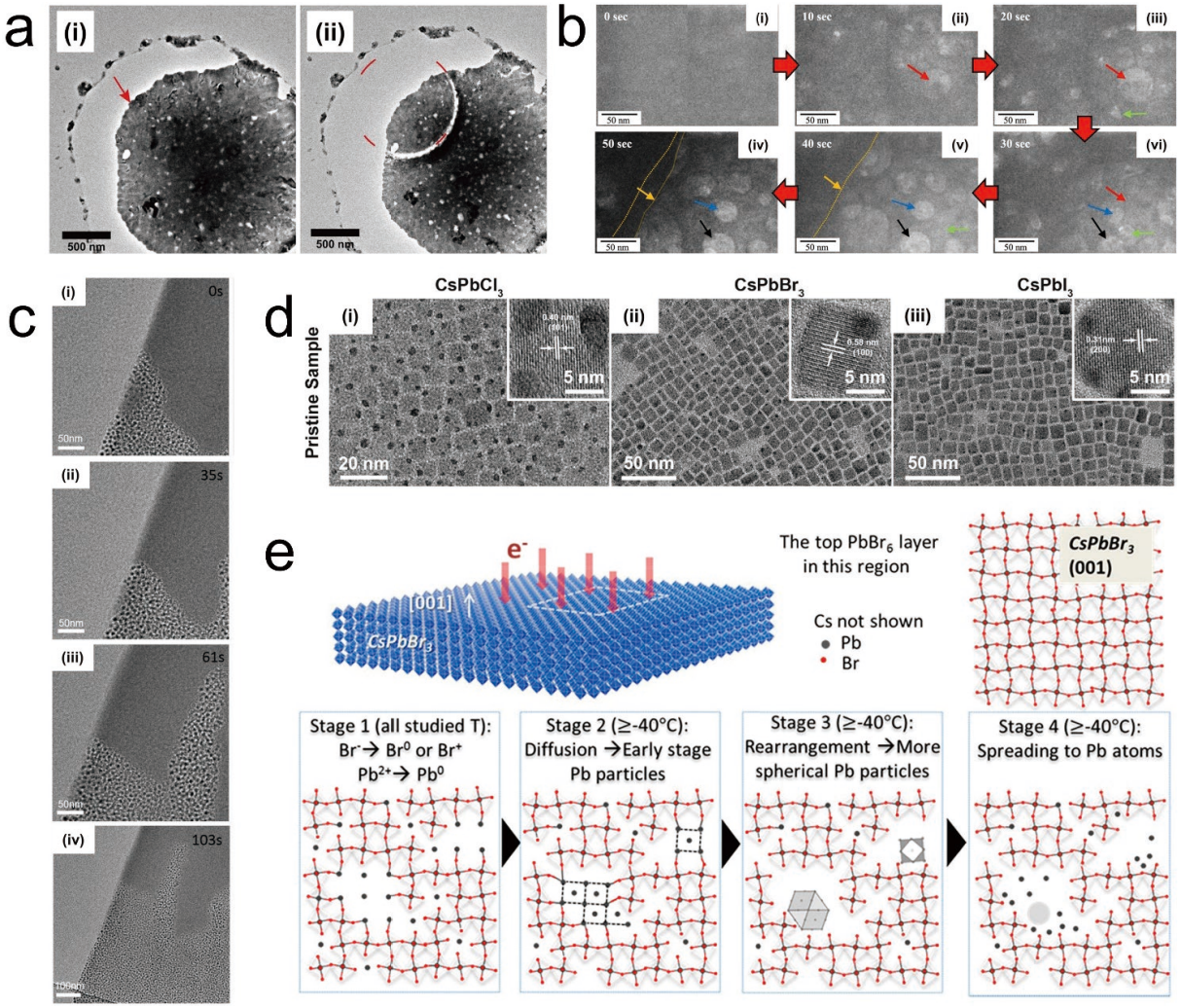

Fig. 2. (Color online) (a) Electron beam irradiation damage observed in free-standing $MAPbI_3$ films. (i, ii). TEM images recorded initially and after the irradiation (9870 e/(Å^2·s) for ~2 min), respectively[47]. (b) Time-series of TEM images on $MAPbI_3$ single crystal showing the electron beam damage from 0 to 50 s, where bubble-like morphology (colored arrows) emerged and grew[49]. (c) Time-series of TEM images obtained on BA_2PbBr_4 nanosheets[53]. (d) TEM images of the (i) $CsPbCl_3$, (ii) $CsPbBr_3$ and (iii) $CsPbI_3$ QDs where "dark spots" present at the QD corners indicated irradiation damage[54]. (e) Schematic illustration of $CsPbBr_3$ degradation pathway[56].

quickly precipitated and the nanosheets were amorphized even at low magnification, as shown by time series TEM in Fig. 2(c)[53].

Irradiation damage is also frequently noticed in all-inorganic halide perovskites. Taking $CsPbX_3$ for example, Li *et al.* found that even short time of exposure could cause "dark spots" to emerge at the corners of the quantum dots (QDs) when imaging $CsPbCl_3$, $CsPbBr_3$ and $CsPbI_3$ QDs as shown in Fig. 2(d)[54]. The emerged "dark spots" were confirmed as PbX_2 nanoparticles, as reported in other related works as well[55–58]. Further analysis inferred that the irradiation-induced precipitation of PbX_2 was due to the surface defects on nanoparticles, and could be effectively suppressed by ZnX_2/hexane treatment which "repaired" the halogen ion defects[54]. Similarly, Wang *et al.* reported a layer-by-layer decomposition of $CsPbBr_3$ which also started from the surface, confirming the impact of surface passivation[58]. Continuous irradiation may further cause phase separation and lead to amorphization in nanocrystals as revealed by Funk *et al.*[59]. Similarly, Dang *et al.* studied $CsPbX_3$ 2D nanosheets and 1D nanowires by HAADF-STEM imaging, and also reported the precipitation of nanoparticles, at low dose of 400 e/Å^2 under both 80 and 200 kV[56]. The degradation mechanism of $CsPbBr_3$ under electron beam irradiation was proposed to be dominated by decomposition coupled with knock-on damage: the incident electrons first led to the desorption of halogen ions and reduced Pb^{2+} to Pb^0 partially; Pb^0 then migrated and aggregated to form precipitation of Pb; finally, the $CsPbBr_3$ collapsed and became amorphized, as illustrated in Fig. 2(e).

More recently, Pb-free halide perovskites with a double perovskite structure are being developed, such as $Cs_2AgBiBr_6$, $Cs_2CuSbCl_6$, $Cs_2AgInCl_6$. Zhou *et al.* synthesized $Cs_2CuSbCl_6$ nanoparticles, and Cruetz *et al.* synthesized $Cs_2AgBiCl_6$, $Cs_2AgBiBr_6$ and $CsAgBiI_6$ nanoparticles, and they were all characterized by TEM[60, 61]. However, irradiation damage was not alleviated in these structures, if not worse. Quick precipitation of nanoparticles and decomposition was also noticed in these materials even at extremely low dose. It was proposed that the degradation was initially induced by the Knotek-Fabel effect at the surface, and was then followed by decomposition into $Cs_3Bi_2Br_9$, $BiBr_3$, $CsAgBr_2$ and AgBr. When the electron beam dose rate was less than 2 e/(Å^2·s), the structure could be maintained for about 4 min as confirmed from electron diffraction. Alternatively, $Cs_2AgBiBr_6$ lattice image could be ob-

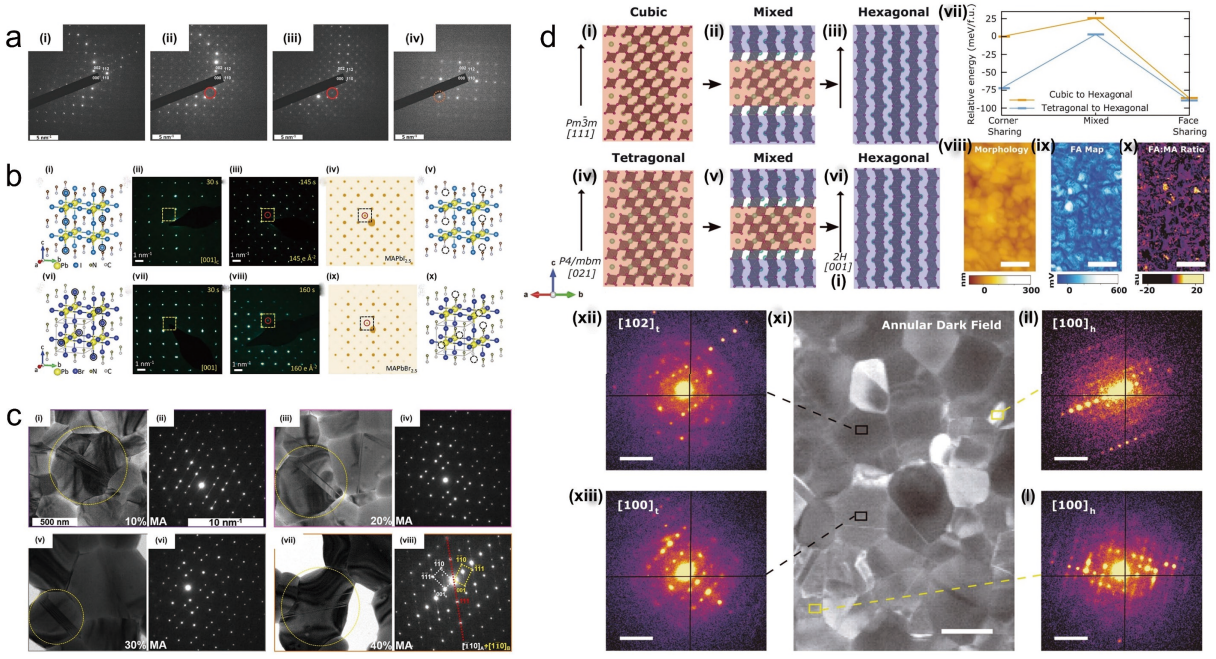

Fig. 3. (Color online) (a) Degradation of $MAPbI_3$ studied using SAED taken from a near-<$1\bar{1}0$>$_t$-oriented grain: i) the initial, pristine phase and ii) after 1 min (total dose per area of ≈1 × 10^2 e/Å^2), iii) 2 min (total dose per area of ≈2 × 10^2 e/Å^2), iv) 18 min (total dose per area of ≈2 × 10^3 e/Å^2) of weak electron beam exposure (≈2 e/Å^2)[46]. (b) Degradation in $MAPbX_3$ by forming superstructured intermediate phase: i) atomistic structure of tetragonal $MAPbI_3$; ii) electron diffraction (ED) pattern along the $[001]_c$ direction; iii) the observed ED of superstructure phase; iv) the simulated ED of superstructure phase $MAPbI_{2.5}$; v) the corresponding atomistic structure; vi) atomistic structure of $MAPbBr_3$; vii) ED pattern along the [001] direction; viii) the observed ED pattern with additional reflections; ix) the simulated ED of superstructure phase $MAPbBr_{2.5}$; x) the corresponding atomistic structure with ordered bromine vacancies[69]. (c) TEM images and [110] oriented-SAED patterns taken from grain highlighted in yellow circles from $FAPbI_3$ films with (i, ii) 10% MA, (iii, iv) 20% MA, (v, vi) 30% MA, (vii, viii) 40% MA[78]. (d) Stabilization of photoactive perovskites against degradation by tilted octahedral, as illustrated by structural model (i–vi), calculated energy difference (vii), AFM-IR characterization (viii–x), and TEM imaging (xi) with corresponding SAED (xii–l)[79].

tained under a single exposure with a dose rate of less than 281 e/(Å^2·s) using conventional HRTEM[62].

It is generally accepted that the electron dose and dose rate have the most influence on the degradation of halide perovskites under electron irradiation, yet it is interesting to discuss the impact of accelerating voltage, i.e. beam energy. In the damage caused by electron beam radiation, it is generally believed that there are three types of radiation damage mechanisms, that is, knock-on damage, radiolysis, and rise of local temperature caused by phonons excited by electron beam radiation[63, 64]. As the latter two factors are more related to electron dose, the first factor is closely related beam energy. Recently, Cai *et al.* calculated the knock-on damage on hybrid halide perovskites using first principle, and showed that iodine is only knocked-out when accelerating voltage is higher than ~250 kV[65]. This is in contrast to experimental results, where low kV has been performed to study the hybrid perovskites where degradation is not noticeably reduced[56, 66, 67]. Therefore, it is a strong evidence that radiolysis dominates the degradation of halide perovskites under electron beam irradiation, and low-dose is vital for TEM characterization.

3. Degradation mechanism and defects identification of halide perovskite using electron diffraction

Due to the beam-sensitivity of halide perovskites, selected area electron diffraction (SAED) with the advantage of low dose, has become a powerful tool to study the degradation mechanism and intrinsic microstructures of halide perovskites.

Rothmann *et al.* acquired SAED time-series through continuous irradiation to study the degradation of $MAPbI_3$ single crystal as shown in Fig. 3(a)[46]: (1) the disappearance of intrinsic twinning structures; (2) the generation of $\sqrt{2} \times \sqrt{2}$ superlattices; (3) the disappearance of the superlattices and the resize of diffraction patterns; (4) the decrease of I : Pb from 3 : 1 to 2 : 1, suggesting the formation of PbI_2. Degradation mechanism was proposed as: $CH_3NH_3PbI_3 \xrightarrow{e^-} (-CH_2-) + NH_3 \uparrow + HI \uparrow + PbI_2$, where the volatility of NH_3 and HI first led to the twisting of $[PbI_6]$ octahedra, thereby resulting in intermediate phase as $\sqrt{2} \times \sqrt{2}$ superlattices. It is interesting to notice that the degradation of $MAPbI_3$ was related to the total dose rather than dose rate. Under the accelerating voltage of 200 kV, a dose of <100 e/Å^2 can cause the degradation of $MAPbI_3$ to PbI_2 through the above-mentioned process.

Similar to Rothmann's work, Chen *et al.* also studied the degradation process of $MAPbI_3$ through SAED time series[68]. Whilst degradation from $MAPbI_3$ to PbI_2 was also observed and confirmed, the generation of superstructure diffraction patterns was interpreted due to the formation of ordered halide vacancies, thereby resulting in $MAPbI_{2.5}$ intermediate phase. Moreover, the effects of electron dose and dose rate under the accelerating voltage of 300 kV were compared: at a dose rate of 0.5 e/(Å^2·s), $MAPbI_{2.5}$ mesophase appeared in

303 s, and at a dose rate of 1 e/(Å^2·s), $MAPbI_{2.5}$ mesophase appeared in 73 s, indicating that the degradation of $MAPbI_3$ under electron beam irradiation was not only related to the total dose, but also to the dose rate, and thus a higher dose rate might accelerate the degradation of $MAPbI_3$. The same group of authors continued to study the degradation process of $MAPbBr_3$ by SAED and reported a similar degradation process, proposing a general degradation mechanism for $MAPbX_3$ as halogen ion desorption → formation of ordered vacancies → formation of $MAPbX_{3-x}$ mesophase → precipitation of PbX_2", as shown in Fig. 3(b)[69]. Similar degradation pathways had been generally recognized in oxide perovskites, but it was first proposed in halide perovskites[70, 71]. More recently, similar degradation mechanism was reported in all-inorganic perovskite of γ-$CsPbIBr_2$ as well, where an intermediate phase [e.g., $CsPb_{(1-x)}(IBr)_{(3-y)}$] with a superstructure of ordered vacancies was formed, followed by reduction from Pb^{2+} to Pb^0 and thus precipitation of Pb nanoparticles[72].

SAED is also used to study the degradation mechanism of 2D nanosheets due to their extreme beam-sensitivity. Yuan *et al.* studied the structural changes of $BA_2FAPb_2I_7$ and $BA_2MAPb_2I_7$ under electron beam irradiation by recording SAED time series, and proposed the degradation mechanism as following: organic ligands between the nanosheets were firstly destroyed by the electron beam; the organic moieties and [$PbBr_6$] octahedra were then damaged, resulting in the rapid collapse of the structure[73]. The proposed degradation mechanism was confirmed by Nie *et al.*: by investigating the morphology changes and SAED patterns of BA_2PbBr_4 nanosheets exposed to ultraviolet and white light, the authors found that the organic ligands between nanosheets were most sensitive to light irradiation; further exposure resulted in the tilt of [$PbBr_6$] octahedra and then amorphization.

In addition to the study of degradation mechanism, SAED has been employed to characterize the microstructures of halide perovskites in a damage-free manner. Rothmann *et al.* discovered the existence of nano-twinning in $MAPbI_3$ single crystal by SAED[38]. Li *et al.* studied the intergrain planar defects in $MA_{1-x}FA_xPbI_3$ perovskites by low dose electron diffraction, and found that the as-fabricated solar cell performance correlated empirically with the density and structure of $\{111\}_c$ planar defects and $\{112\}_t$ twin boundaries[74]. Gao *et al.* obtained SAED diffraction patterns of BA_2PbI_4 nanosheets with different structures, and obtained the lattice image of 2D nanosheets through filtering and inverse fast Fourier transform[75]. For all-inorganic perovskites, Pan *et al.* revealed the B-site cations disorder in $Cs_2AgBiBr_6$ using electron diffraction[76]. Luo *et al.* combined SAED and nano-diffraction to reveal a partial ordering of Ag/Na cations in $Cs_2Ag(Na)InCl_6$ single crystal[77]. Using a nano-beam with a diameter of ~5 nm (equal to current density of ~1.6 pA/cm^2) and a dwell time of 0.1 s, the authors demonstrated damage-free scanning over the sample for several minutes. Pham *et al.* unraveled the influence of CsCl/MACl on stabilizing cubic α-$FAPbI_3$ phase and minimizing twinning/stacking faults through electron diffraction as shown in Fig. 3(c)[78]. More recently, Doherty *et al.* revealed that α-$FAPbI_3$ stabilized by Cs and MA cations alloying had octahedral tilting of ~2°, which imparted the phase stability by frustrating transitions from photoactive to hexagaonal phases. Such minor tilting was neglected by bulk characterization such as XRD, but was resolved by electron diffraction, as shown in Fig. 3(d)[79].

4. Emerging TEM approaches for halide perovskites at atomic resolution

Driven by the urgent need to understand the structure-properties relationship of halide perovskites, novel approaches on both hardware and methodology are being developed to overcome the limits opposed by electron dose, and to further push the spatial resolution down to atomic scale.

With regard to the degradation mechanism of halide perovskites under electron irradiation, it is generally accepted that: (1) the electron dose and dose rate are dominating the irradiation process, and therefore low-dose imaging is essential; (2) the disassociation of organic ligands and halide ions is the first to trigger decomposition of halide perovskites. In light of these understandings, various methods have been proposed to push HRTEM imaging of halide perovskites towards atomic scale, including: (1) deposition or coating of carbon film to alleviate the radiolysis damage; (2) improvement on detectors such as direct electron detector to enable ultra-low-dose imaging; (3) developments of low-dose imaging techniques such as exit-wave reconstruction, ptychography, and iDPC etc.

Above-mentioned techniques have demonstrated to be successful in resolving pristine structures of halide perovskites at atomic scale. Yu *et al.* revealed the microstructure of $CsPbBr_3$ by defocus series at a low dose rate of ~100 e/(Å^2·s) under accelerating voltage of 80 kV[41]. As shown in Fig. 4(a), nano-domain with the co-existence of cubic phase and orthogonal phase was demonstrated. Brennan *et al.* further applied the same approach onto $CsPbBr_3$ nanocubes and reported a size dependency on the crystal phases[80]. Alternatively, Zhang *et al.* employed a direct-detection electron-counting camera to obtain the first atomic resolution image of $MAPbBr_3$ at a total dose of only 11 e/Å^2, revealing nano-domain structure where the MA^+ cations were ordered locally in the single crystal, as shown in Fig. 4(b)[39, 81]. Chen *et al.* also used direct-detection electron-counting camera to investigate the decomposition pathway of $MAPbI_3$ at atomic scale, where the intermediate phase of $MA_{0.5}PbI_3$ with locally ordered vacancies was successfully imaged[82]. Alternatively, iDPC has been demonstrated to be helpful in revealing the atomic structures of halide perovskites: an early iDPC-STEM attempt for the investigation of $MAPbBr_3$ was performed by Song *et al.*, enabling low-dose imaging at atomic scale[81]; more recently, Qiao *et al.* demonstrated the magnified iDPC-STEM image could clearly distinguish the atomic distributions of Cs, Pb, and Br from monodispersed $CsPbBr_3$ nanocrystals, as encapsulated and stabilized in metal-organic framework[83]. Recently, ptychography has been applied to image halide perovskites due to its advantage of low dose. As shown in Fig. 4(c), the presence of Br was revealed at atomic scale[84]. It is interesting to mention that pulsed-beam TEM has been demonstrated on studying $MAPbI_3$, where the dose could be controlled as low as 0.001 e/Å^2[85]. Although the spatial resolution is rather low compared to HRTEM, it offers a possibility for damage-free study of halide perovskites.

Thanks to the development of low-dose imaging tech-

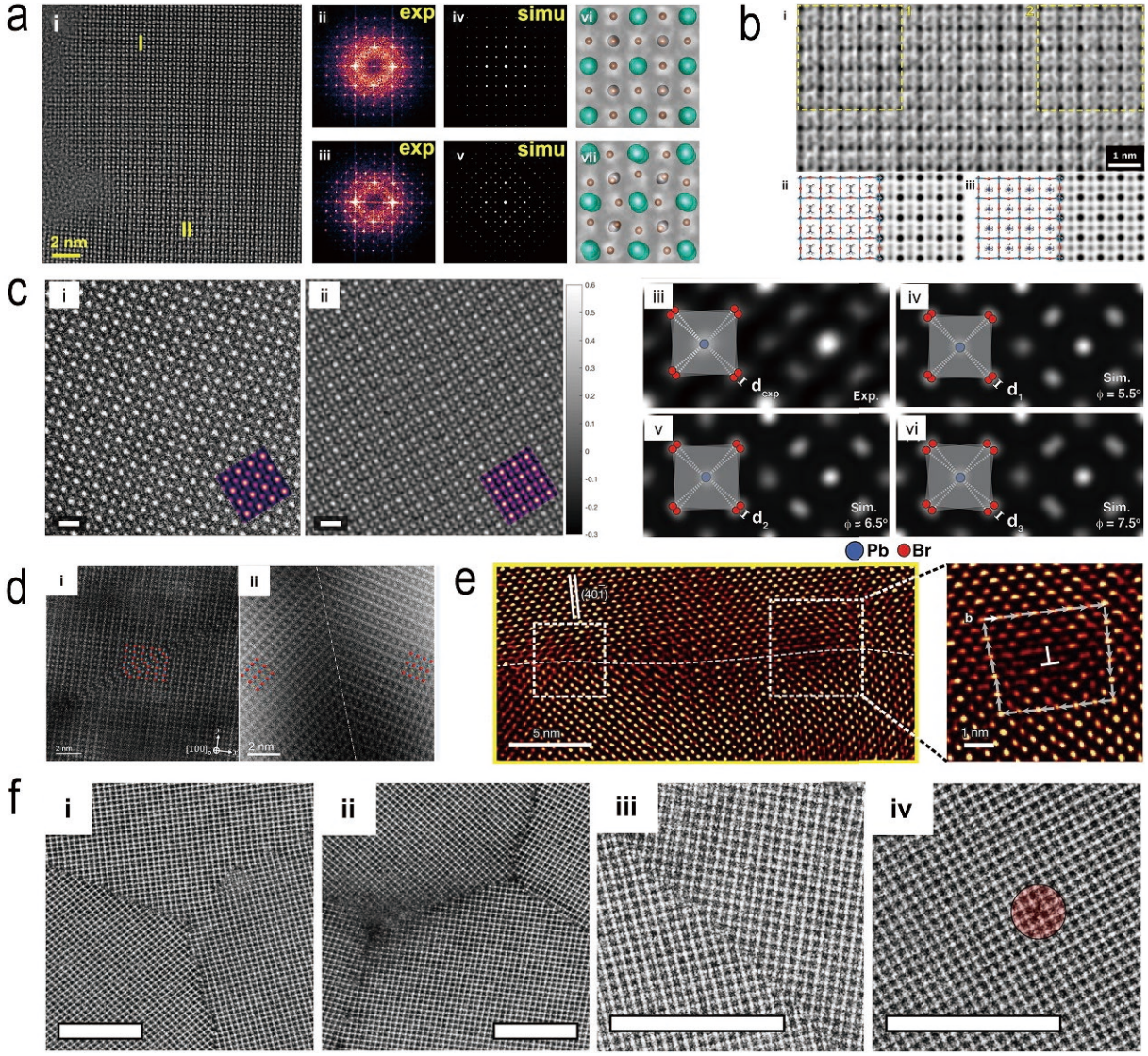

Fig. 4. (Color online) (a) HRTEM of $CsPbBr_3$ nanocrystals (i) where the coexistence of cubic and orthorhombic phases were demonstrated by FFT patterns (ii, iii), simulated diffraction patterns (iv, v), and illustrated structure (vi, vii)[41]. (b) CTF-corrected denoised HRTEM image (i) of $CH_3NH_3PbBr_3$ with different CH_3NH_3 orientations, where (ii, iii) the structural model (left) and the simulated projected potential map (right) corresponding to region 1 and 2 in (i), respectively[39]. (c) Ptychography reconstructed image of $CsPbBr_3$, with the scale bar of 5Å[84]. (d) Atomic-scale structures of intragrain stacking-fault (i) and twinning interfaces (ii) obtained on orthorhombic $FA_{0.5}Cs_{0.5}PbI_3$ grains along the [100] projection direction[86]. (e) Atomically resolved interface at the $(2T)_2$ PbI_4–$(2T)_2$ PbI_4–$(2T)_2$ $PbBr_4$ heterostructure[87]. (f) Butterworth-filtered LAADF-STEM images of grain boundaries (i), triple junctions (ii), grain boundary (iii) and aligned vacancy defects indicated by red circle (iv), obtained from a 30-nm-thick film of $FAPbI_3$[67].

nique, defects in halide perovskites have been imaged in detail as never before. Cai *et al.* recently succeeded in imaging grain boundaries of $MAPbI_3$ PSCs at atomic scale by developing a coating approach onto FIB-prepared cross section, as shown in Fig. 4(d)[86]. The carbon coating can significantly inhibit the loss of volatile substances such as CH_3NH_2 and halogens. It was suggested by Chen *et al.* that depositing carbon film with a thickness of ~6–10 nm on $MAPbI_3$ could increase its tolerance against electron irradiation by nearly 10 times[69]. On the other hand, Shi *et al.* successfully resolved the atomic structure on $(2T)_2$ PbI_4–$(2T)_2$ PbI_4–$(2T)_2$ $PbBr_4$ heterojunction nanosheets, through continuous exposure at extremely low dose and subsequent superposition of time series[87]. In this manner, HRTEM images with a high signal-to-noise ratio were obtained under a total dose of only 9.2 e/Å^2, and defects at the heterojunction interface were revealed at atomic scale as shown in Fig. 4(e). Recently, Jung *et al.* revealed the growth of polytypic PbI_2 on the surface of 2D Ruddlesden-Popper halide perovskites $BA_2MA_2Pb_3I_{10}$, where a sequential layer-by-layer degradation from perovskites to PbI_2 was imaged at atomic scale[88]. $CsPbBr_3$ nanocrystals were also studied by HAADF-STEM, where Ruddlesden-Popper stacking fault was revealed by a beam current of 50 pA at an accelerating voltage of 300 kV[89, 90]. The author mentioned that a short dwell time of 3–6 μs can suppress irradiation damage. Additionally, Rothmann *et al.* used low-angle annular dark field STEM (LAADF-STEM) to study $FAPbI_3$ thin films, and successfully imaged grain boundaries at atomic scale as shown Fig. 4(f)[67]. It was suggested by the authors that LAADF-STEM could effectively lower the beam damage on halide perovskites, and therefore might find more applications in resolving atomic structure of beam-sensitive materials.

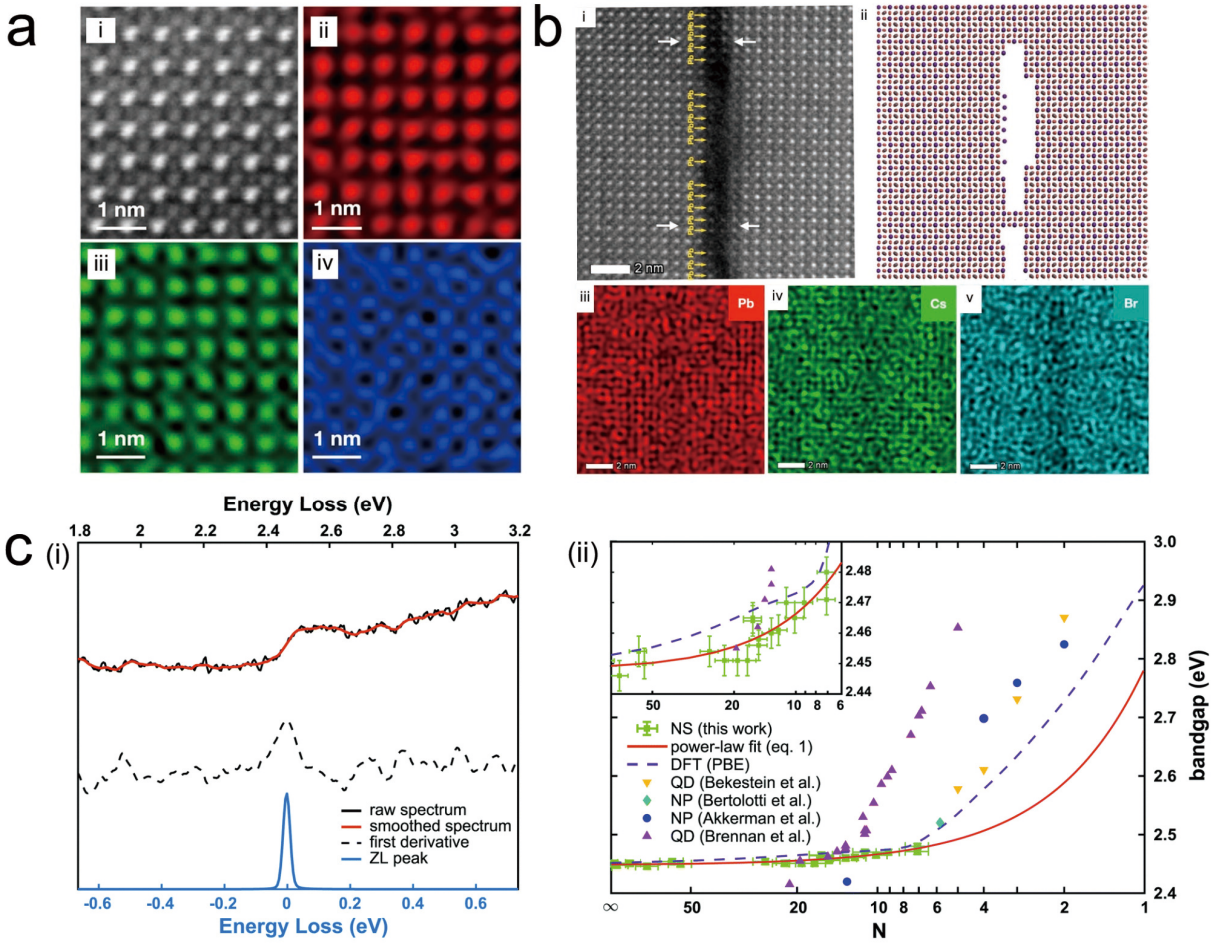

Fig. 5. (Color online) (a, b) Atomically resolved HAADF-STEM images and corresponding EDX-mappings of $CsPbBr_3$ nanoplates[92]. (c) STEM-EELS from a $CsPbBr_3$ nanosheet to determine bandgap, where (i) demonstrates measured data and (ii) shows as-calculated bandgap value[93].

5. Chemical mapping of halide perovskites using STEM-EDX or STEM-EELS

Due to the beam sensitivity, elemental mapping of halide perovskites has been a standing issue for microstructure investigations. Large dose is often required to obtain enough counts for either EDX-mapping or EELS-mapping, which exceeds the degradation threshold of halide perovskites. Although chemical mapping has been reported in many halide-perovskites study, it is also known that the instability of halide perovskites during beam irradiation thus leads to the reliability of elemental mapping, questioning whether the mapped results reflect the pristine structure. Therefore, novel approaches have been proposed to enable the elemental mapping down to atomic scale.

Kosasih *et al.* performed a systematic study on the evaluation of STEM-EDX quality demonstrated on state-of-art triple-cation, double-halide perovskite with a nominal stoichiometry of $Cs_{0.06}FA_{0.79}MA_{0.15}Pb(I_{0.85}Br_{0.15})_3$[91]. The acquisition parameters were systematically varied to evaluate the relationship between electro dose, data quality and irradiation damage. It was found that the iodine content decreased exponentially with electron dose, and thus called attention to the interpretation of STEM-EDX mapping results.

In order to minimize electron damage, Liu *et al.* recently fabricated a highly-beam-stable $CsPbBr_3$ nanoplates through an interface-assisted regrowth method using cyanamide[92]. By defect-healing self-assembly/regrowth processes and surface passivation by cyanamide molecules, the as-prepared $CsPbBr_3$ was demonstrated to be highly stable against electron beam irradiation and thus achieved elemental mapping at atomic resolution, as shown in Figs. 5(a) and 5(b). The stability improvement as shown in this work demonstrates that the beam damage starts from the surface, where surface passivation and defect-healing can effectively suppress the radiolysis damage, although further experiments are needed to check the universality of this method.

On the other hand, STEM-EELS has been demonstrated on orthorhombic $CsPbBr_3$ to determine bandgap as shown in Fig. 5(c)[93]. Care was taken in spreading the electron dose for the EELS experiments so to minimize irradiation damage, and the beam current was set to be <5 pA. Meanwhile, the spectra were collected by summing up individual datapoints from spectrum images acquired over a large sample area. By this mean, the spectra with a high S/N ratio could be collected for accurate bandgap determination. Interestingly, bandgap increase was found at nanoplates with thickness below 10 nm, and thus confirming 1D confinement in nanosheets. More studies using EELS or EDX are foreseen to contribute to the studies of halide perovskites.

6. Fast-developing cryogenic TEM for halide perovskites

Cryogenic TEM (cryo-TEM) has been developed rapidly in

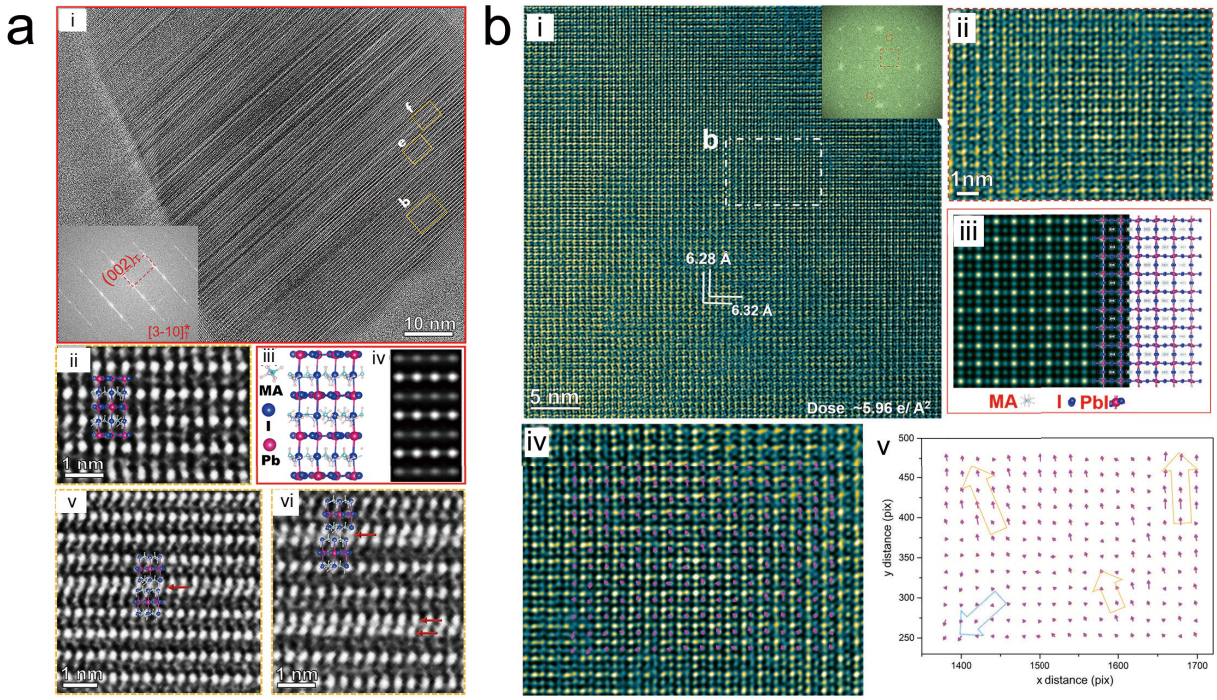

Fig. 6. (Color online) (a) Stacking faults observed in a $MAPbI_3$ with corresponding FFT patterns as inset (i), and corresponding magnified HRTEM (ii, v, vi) with structural model (iii) and (iv) the simulated HRTEM image[96]. (b) Atomically resolved-cryo-TEM image of aged $MAPbI_3$ collected at a low dose condition (electron dose, ~5.96 e/Å^2), with corresponding enlargement (ii, iv), structural model (iii) and polarization map (v)[40].

recent years. Beyond life science, its development has also offered opportunities to materials science, particularly to those too sensitive for conventional HRTEM and related spectroscopy[94]. Growing applications are found for energy-related materials in past few years, and halide perovskites are benefitting from cryo-TEM as well[95].

Li *et al.* combined the cryogenic temperature with direct electron detector dedicated for low-dose imaging, and successfully obtained HRTEM of $MAPbI_3$ and $MAPbBr_3$ under the dose of 12 e/Å^2 and 46 e/Å^2[48]. Zhu *et al.* investigated the $MAPbI_3$ single crystal at atomic scale using cryo-TEM, where electron dose rate was kept at ~47 e/(Å^2·s) for about 2 s[96]. Defects of surface steps and high density of stacking faults were revealed and correlated to the optoelectronic behavior of charge separation and carrier recombination (Fig. 6(a)). The same group further studied the formation of halide perovskites in the initial nucleation stage using low-dose imaging by cryo-TEM, as demonstrated on both $MAPbI_3$ and $MAPbBr_3$ respectively (Fig. 6(b)). A growth pattern from initially stacked slices towards a perfect single crystal structure was revealed, proposing a so-called twist-to-untwist structural evolution[40, 97]. Low-temperature imaging was also applied to all-inorganic perovskites such as $CsPbBr_3$[98]. The degradation mechanism was proposed as following: the migration and aggregation of Pb were suppressed at low temperature, and degradation was then dominated by the desorption of halogen ions induced by incident electrons, which led to decomposition products of CsBr, CsPb and $PbBr_2$ nanoparticles; further irradiation caused the formation and growth of pores and thus destroyed the structure. Additionally, it is interesting to mention that cryo-FIB has been applied to prepare specimen for atom probe tomography[99]. More recently Zhou *et al.* reported cryo-FIB preparation of a $MAPbI_3$ single crystal film solar cell cross-section, enabling high quality microstructural investigation by electron diffraction[100]. Damage-minimized sample preparation by cryo-FIB is thus expected to find more applications in the cross-section preparation of PSCs for more reliable microstructural investigation.

Nevertheless, it should be noted that the use of cryogenic temperature for halide perovskites imaging remains an open issue. It was reported by Rothmann *et al.* that low temperature could not alleviate irradiation damage but led to rapid amorphization of $MAPbI_3$[46]. Similar results were reported on $FAPbI_3$ thin films, where both room-temperature and cryogenic conditions were performed for imaging, but beam sensitivity was not noticeably reduced in the cryogenic conditions[67]. Therefore, detailed studies on the imaging conditions and degradation pathways in the cryogenic conditions are still needed towards further developments.

7. *In-situ* TEM dedicated to reveal degradation of halide perovskites under environmental conditions

Although much progress has been achieved in resolving the microstrure of as-grown halide perovskites or as-fabricated photovoltaic devices from nanoscale down to atomic scale, there is an urgent need to study the structural evolution of halide perovskites based devices under external stimuli such as light, heat and moisture so to understand the degradation of perovskites under environmental factors[101–104]. *In-situ* TEM is thus considered as a powerful tool to this end, and has achieved significant progress in the past few years[3, 105, 106].

The thermal stability of halide perovskites can be studied by *in-situ* heating in TEM. As demonstrated by Divitini *et al.*, the morphology and chemical composition change of $MAPbI_3$-based PSC during elavating temperature (up to

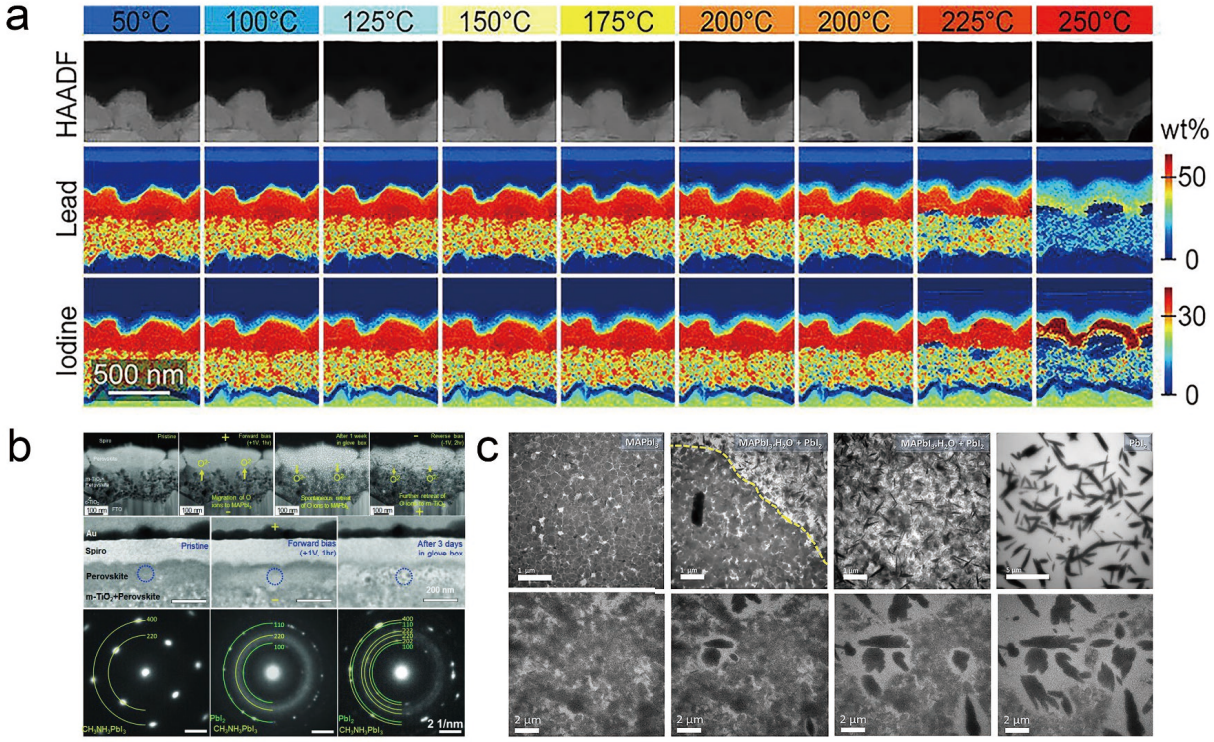

Fig. 7. (Color online) (a) *In-situ* heating of $MAPbI_3$ based PSCs up to 250 °C, where the temperature evolution of morphology change and elemental migration was monitored by HAADF-STEM images and EDX mappings. The same scale bar applies to all panels[42]. (b) *In-situ* electrical biasing on $MAPbI_3$, where morphology and structure change was monitored by HAADF-STEM, TEM and SAED, respectively[109]. (c) *In-situ* TEM showing the impact of controlled humidity on the conversion of $MAPbI_3$ into $MAPbI_3{\cdot}H_2O$ and finally PbI_2, using liquid cell[112].

250 °C) was monitored using a FIB prepared cross-section (Fig. 7(a))[42]. Migration of I and Pb was revealed and correlated to the synthesis condition. Seo *et al.* further compared the thermal responses of $Cs_x(FA_yMA_{(1-y)})_{(1-x)}Pb(I_zBr_{(1-z)})_3$ to $MAPbI_3$ PSCs using *in-situ* heating, and found that $MAPbI_3$ degraded rapidly by forming particles and voids, whereas FA-based PSCs is more heat-resistant. Similarly, the thermal stability of inorganic perovskites has been demonstrated on $CsPbBr_3$, and found a superb stability up to 690 K[107].

The impact of curent–voltage stimulus on perovskites degradation can be investigated by *in-situ* biasing. $MAPbI_3$-based PSC was prepared into cross section and subjected to biasing in TEM by Jengros *et al.*[108]. Degradation was identified particularly at the positively biased $MAPbI_3$ interface, where iodide migrated into the transport layer and volatilized, resulting in the nucleation of PbI_2 nanoparticles and voids. $MAPbI_3$ interface with TiO_2 as electron transport layer was further studied using *in-situ* biasing combined with HRTEM and STEM-EELS (Fig. 7(b))[109]. It was found that positive bias led to oxygen diffusion into the $MAPbI_3$ layer accompanied with performance degradation, wheras a negative bias could remove oxygen ions from $MAPbI_3$ and partially restored the performance. Kim *et al.* observed amorphization of perovskite layer by *in-situ* biasing as induced by ion migration, whereas the bias-introduced degradation could be healed by heating at 50 °C[110]. More recently, an *in-situ* electrical probing and light illumination through an optical fiber was applied to study the optoelectronic and photovoltaic properties on different crystal facets of $CsPbBr_3$[111]. This work demonstrated a possibility of studying light-introduced degradation of perovskites.

Last but not least, the moisture-induced degradation was recently studied using in-operando liquid cell TEM (Fig. 7(c))[112]. A live visualization from meso-to-nanoscale transfomration between prototypical $MAPbI_3$ and water molecules was presented: intermediate phase of $MAPbI_3{\cdot}H_2O$ was first formed upon exposure to humidity, and was subsequently decomposed into PbI_2 crystals through dissolution/recrystallization. In addition, *in-situ* liquid cell TEM has been used to study the nucleation of pervoskites as demonstrated on $MAPbI_3$ as well, providing useful reference for understanding the intriguing chemical and physical properties of halide perovskites [113].

8. Conclusions and perspective

This review summarizes the recent progress of advanced TEM characterization for halide perovskites. The main conclusions are as following.

(1) Due to the presence of halogen ions and organic moieties, halide pervoskites are extremely sensitive to electron beam irradiation. Conventional TEM causes degradation in almost all halide perovskite structures, showing "artifacts" and damage such as the generation and expansion of holes, grain boundary cracking, and nanoparticle precipitation. Although the degradation mechanism under electron beam interaction remains unclear, it generally follows the pathway of "electron beam incidence → organic moieties and/or halogen ion desorption → defect generation and expansion → lattice collapse and amorphization → PbI_2 or Pb precipitation". Both electron dose and dose rate have impact on the degradation. The understanding of degradation is essential, as it calls attention to the interpretation of TEM results and ultra-care in per-

Table 1. Summary of TEM characterization details for $MAPbI_3$ and related structures. No damage or little damage was reported unless specified in the table.

Perovskite chemistry	Specimen morphology	TEM method	Special characterization tools	Accelerating voltage	Dose ($e/Å^2$)	Dose rate ($e/(Å^2 \cdot s)$)	Damage evaluation and additional note	Corresponding figure in this review	Year and reference
$MAPbI_3$	Freestanding thin film	SAED		200		1			2017, [38]
$MAPbI_3$	Single crystal	SAED		300	151 73 4	0.5 1 2	Upper dose limit at mentioned dose rate before damage		2018, [68]
$MAPbI_3$	Freestanding thin film	SAED		200	<100	2	Exposure > 60 s at the mentioned dose rate led to damage	3(a)	2018, [46]
$MAPbI_3$	Single crystal	SAED		300	<99	1	Ordered vacancy was noticed at 145 $e/(Å^2 \cdot s)$	3(b)	2020, [69]
$MAPbI_3$	Single crystal	SAED	Cryogenic temperature	300	<30				2020, [71]
			25	300	30–41		Damaged at the dose of 475 $e/(Å^2 \cdot s)$		
			90	300	38		Damaged at the dose of 523 $e/(Å^2 \cdot s)$		
				80	13–16				
$MA/FAPbI_3$	Freestanding thin film	SAED		200		2			2021, [74]
$MAPbI_3$	Single crystal	TEM		200	4–8	1			2019, [50]
$MAPbI_3$	Freestanding thin film	TEM		200	9870		Damaged	2(a)	2019, [47]
$MAPbI_3$	Nanoparticles	TEM	Pulsed-beam TEM	200	10	0.001			2020, [85]
$MAPbI_3$/ $FAPbI_3$	Freestanding thin film	LAADF-STEM		200	66		Undamaged	4(f)	2020, [67]
					200		Change in structure was noticed		
					600		Damaged		
$MAPbI_3$	Nanowire	HRTEM	Cryo-TEM	300	12				2019, [48]
$MAPbI_3$	Nanoparticles	HRTEM	Cryo-TEM	300	<100			6(a)	2020, [96]
$MAPbI_3$	Nanoplatelets	HRTEM	Cryo-TEM	300	5.96	2	Lattice changed noticed at accumulated dose of 23.64 $e/Å^2$	6(b)	2021, [40]
$MAPbI_3$	–	HRTEM	Direct electron detector	300	5.95		Superstructure was noticed		2021, [81]
$MAPbI_3$	Single crystal	HRTEM	Direct electron detector	300	1		MA loss at the mentioned dose		2021, [82]
				300	<28		MA loss reached a balanced state between ~10.5 and 28.0 $e/Å^2$		
$MAPbI_3$	FIB-milled PSC cross section	HAADF-STEM and STEM-EDX	*In-situ* heating ~150℃	200				7(a)	2016, [42]
$MAPbI_3$	FIB-milled PSC cross section	HAADF-STEM, STEM-EDX	*In-situ* biasing	300			Beam current of 50 pA was used		2016, [108]
$MAPbI_3$	Nanoparticles	TEM	Liquid cell	200		<90	Dose rate of >125 $e/(Å^2 \cdot s)$ causes damage		2016, [113]
$MAPbI_3$	FIB-milled PSC cross section	TEM	*In-situ* biasing	300	2–3	1–10		7(b)	2018, [109]
$MAPbI_3$	Nanoparticles	TEM	*In-situ* humidity	200		1.3		7(c)	2021, [112]
$FA_{1-x}Cs_xPbI_3$ $FA_{0.5}Cs_{0.5}PbI_3$	FIB-milled PSC cross section	HAADF-STEM		300	1.3×10^4		A thin conformal coating of amorphous carbon about 10 nm thick was deposited to avoid beam damage	4(d)	2022, [86]
$Cs_{0.05}FA_{0.78}MA_{0.17}Pb(I_{0.83}Br_{0.17})_3$	Nanoparticles	Scanning electron diffraction		200	10			3(d)	2021, [79]
$Cs_{0.06}FA_{0.79}MA_{0.15}Pb(I_{0.85}Br_{0.15})_3$	FIB-milled PSC cross section	STEM-EDX		NA	>400		Damaged		2021, [91]

Table 2. Summary of TEM characterization details for $MAPbBr_3$. No damage or little damage was reported unless specified in the table.

Perovskite chemistry	Specimen morphology	TEM method	Special characterization tool	Accelerating voltage	Dose ($e/Å^2$)	Dose rate ($e/(Å^2 \cdot s)$)	Damage evaluation and additional note	Corresponding figure in this review	Year and reference
$MAPbBr_3$	Single crystal	HRTEM	Direct electron detector	300	6–12			4(b)	2018, [39]
$MAPbBr_3$	–	HRTEM	iDPC	300	280				2020, [81]
$MAPbBr_3$	Single crystal	SAED		300	163	<1	Formation of ordered vacancy	3(b)	2020, [69]
				300	63–113	<1			2020, [71]
			Cryogenic temperature	300	81	<1			
$MAPbBr_3$	Nanowire	HRTEM	Cryo-TEM		46				2019, [48]
$MAPbBr_3$	Nanoplatelets	HRTEM	Cryo-TEM	300	4–8	4			2021, [97]

Table 3. Summary of TEM characterization details for all-inorganic $CsPbBr_3$ and related structures. No damage or little damage was reported unless specified in the table.

Perovskite chemistry	Specimen morphology	TEM method	Special characterization tool	Accelerating voltage	Dose ($e/Å^2$)	Dose rate ($e/(Å^2 \cdot s)$)	Damage evaluation and additional note	Corresponding figure in this review	Year and reference
$CsPbBr_3$	Nanosheets	HRTEM	In-line holography, imaging series	80	~8000	100		4(a)	2016, [41]
			Single frame acquisition	80		3800			
$CsPbBr_3$	Nanosheets	HRTEM	<–40 °C	200	500				2017, [98]
		HAADF-STEM	<–40 °C	200	<1800				
$CsPbBr_3$	Nanosheets	HRTEM		200	1140		Pb formation		2017, [56]
$CsPbBr_3$	Nanosheets	CBED	Cryogenic temperature	200				4(c)	2018, [84]
		Ptycho graphy	Direct electron detector	300	1000				
$CsPbBr_3$	Nanoparticles	TEM		200	100–1000				2020, [111]
$CsPbBr_3$	Nanosheets	EELS		60			The beam current was set to <5 pA		2020, [93]
$CsPbBr_3$	Nanoparticles	STEM-EDX		300	9×10^4		Cyanamide passivation to protect surface from damage	5(a)/5(b)	2020, [81] 2021, [92]
$CsPb(Br_{0.8}I_{0.2})_3$	Nanoparticles	HRTEM		0		500	Damaged		2020, [59]
γ-$CsPbIBr_2$	Nanoparticles	HAADF-STEM		300	6000–8000				2021, [72]
$CsPbI_3$	Freestanding thin film	TEM		200	7800		Damaged		2019, [47]

forming TEM characterization.

(2) In order to reduce the irradiation damage, low-dose is vital for halide perovskites' characterization. Electron diffraction has shown to be powerful in resolving the crystal structure and microstructure at low dose. In Table 1–4, we have summarized the imaging conditions as reported in this review according to perovskite chemistry, i.e. $MAPbI_3$, $MAPbBr_3$, all-inorganic $CsPbBr_3$/$CsPbI_3$, and 2D halide perovskites, as an imaging guide for researchers in this field. More importantly, safe dose and damage dose for different perovskite materials are summarized in Fig. 8, where dose limit for imaging is better represented. 2D perovskites are most sensitive to electron dose, whereas $MAPbI_3$ and $MAPbBr_3$ is slightly more robust, and $CsPbBr_3$ has the best tolerance to beam irradiation. It is important to note that dose rate and accelerating voltage also has influence on imaging, and surface treatment to protect the sample can drastically increase the critical dose. Readers are encouraged to refer to the tables and corresponding references for specific notes. Undoubtedly, halide perovskites is one of the most beam-sensitive materials, and researchers are encouraged to carefully design and prepare their TEM experiments in order to achieve meaningful results.

(3) Emerging techniques have been developed to en-

Table 4. Summary of TEM characterization details for 2D halide perovskites. No damage or little damage was reported unless specified in the table.

Perovskite chemistry	Specimen morphology	TEM method	Special characterization tool	Accelerating voltage	Dose (e/Å^2)	Dose rate (e/(Å^2·s))	Damage evaluation and additional note	Corresponding figure in this review	Year and reference
$(2T)_2PbI_4$–$(2T)_2PbBr_4$	Nanosheets	HRTEM		80	9.2	65	Imaging series of 40 ms/frame. Damaged within 1 s	4(e)	2020, [87]
$BA_2MA_2Pb_3I_{10}$ (n = 3)	Nanosheets	HRTEM	Direct electron detector	300	>10^4		Surface damaged with reconstruction		2019, [88]
BA_2PbBr_4	Nanosheets	SAED		300		<1	<1 (spot size 6)	2(c)	2019, [53]
$BA_2FAPb_2I_7$/ $BA_2MAPb_2I_7$	Nanosheets	HRTEM		200	<50				2020, [73]

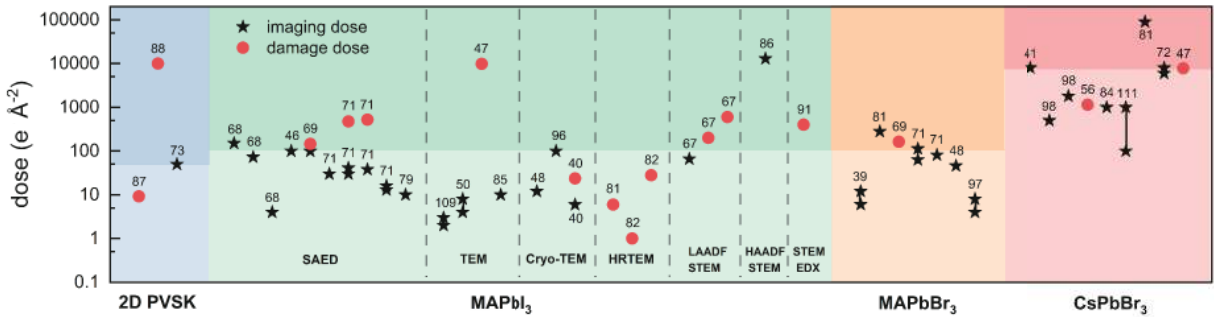

Fig. 8. (Color online) Illustrated summary of safe dose and damage dose for different perovskite materials, plotted in coloured columns. Numbers in the figure correspond to the reference numbers as listed in the tables and references. Shade in each column indicates relatively-safe dose range versus damage-prone dose range. Generally speaking, 2D pvsk is suggested to be imaged below the dose of 50 e/(Å^2·s), $MAPbI_3$/ $MAPbBr_3$ below ~100 e/(Å^2·s), whereas $CsPbBr_3$ can tolerate dose up to more than 1000 e/(Å^2·s).

able atomic-resolution imaging and chemical mapping of halide pervoskites. Low-dose imaging techniques such as exit-wave reconstruction, LAADF-STEM and ptychography has successfully imaged perovskites at atomic scale. The development of hardware such as direct electron detectors have also succeeded in providing atomically resolved structure of halide perovskites. Additionally, the rapid development of cryo-TEM has emerged as a powerful tool to study the halide perovskites and reveal defects such as grain boundaries and surface steps.

(4) *In-situ* TEM under heating, biasing and liquid cell is being developed and applied to study the degradation of halide perovskites under operando conditions. Microstructural change has been revealed with unprecedented details.

Thanks to the rapid developments of emerging TEM techniques, halide perovskites have been resolved down to atomic scale with unprecedented details. Perspectives of TEM characterizations for halide perovskites are proposed as following:

(1) Sample preparation. Imaging techniques such as iDPC, ptychography, and the developments of detectors have paved ways for low-dose imaging, but the bottleneck is sample preparation, particularly for PSC thin films. Conventionally, FIB is used to prepare cross sections, but beam damage of Ga^+ ions can induce significant damage to the sample prior to imaging. The use of cryo-FIB and surface passivation has shown their advantages in alleviating beam damage, and more studies are encouraged.

(2) Development of emerging techniques. Although low-dose imaging and *in-situ* TEM has been demonstrated to reveal the structure-property relationship, the studies are still limited to a few examples. More investigations on different materials and devices are expected.

(3) Interpretation of TEM data. Degradation mechanism has been discussed in this review, emphasizing the impact of electron dose/dose rate on halide perovskite structure. It is clear that only low dose imaging can reveal the halide perovskite structure, although conventional TEM imaging and EDX/EELS study involves large dose, which significantly exceeds damage threshold. Therefore, we call attentions to the interpretation of TEM data as reported in literatures, where attentions should be paid to the imaging condition before correlation to the conclusions.

Halide perovskites are strategically important in the field of energy materials. Along with the rapid development of the materials and related devices, there is an urgent need to understand the structure-property relationship from nanoscale to atomic scale. Much effort has been made in the past few years to address the beam-sensitivity of this particular materials, and more applications of emerging TEM characterizations are foreseen in the coming future, unveiling the structural origin of halide perovskite's unique properties and degradation mechanism under operando conditions, so to assist the design of a more efficient and robust energy material.

Acknowledgements

X.K. and M.S. acknowledge the Beijing Municipal High Level Innovative Team Building Program (IDHT20190503) and the National Natural Science Fund for Innovative Research Groups of China (51621003). X.W. and X.K. acknowledge the National Natural Science Foundation of China (12074017).

References

[1] Jiang Q, Zhao Y, Zhang X W, et al. Surface passivation of perovskite film for efficient solar cells. Nat Photonics, 2019, 13, 460

[2] Lin Y W, Lin G M, Sun B Y, et al. Nanocrystalline perovskite hybrid photodetectors with high performance in almost every figure of merit. Adv Funct Mater, 2018, 28, 1705589

[3] Ran J H, Dyck O, Wang X Z, et al. Electron-beam-related studies of halide perovskites: Challenges and opportunities. Adv Energy Mater, 2020, 10, 1903191

[4] Chen P F, Ong W J, Shi Z H, et al. Pb-based halide perovskites: Recent advances in photo(electro)catalytic applications and looking beyond. Adv Funct Mater, 2020, 30, 1909667

[5] Ye T, Pan L, Yang Y, et al. Synthesis of highly-oriented black $CsPbI_3$ microstructures for high-performance solar cells. Chem Mater, 2020, 32, 3235

[6] Green M A, Ho-Baillie A, Snaith H J. The emergence of perovskite solar cells. Nat Photonics, 2014, 8, 506

[7] Dong Q, Fang Y, Shao Y, et al. Electron-hole diffusion lengths > 175 μm in solution-grown $CH_3NH_3PbI_3$ single crystals. Science, 2015, 347, 967

[8] Shi Z J, Guo J, Chen Y H, et al. Lead-free organic-inorganic hybrid perovskites for photovoltaic applications: Recent advances and perspectives. Adv Mater, 2017, 29, 1605005

[9] Yang Z B, Rajagopal A, Jen A K Y. Ideal bandgap organic–inorganic hybrid perovskite solar cells. Adv Mater, 2017, 29, 1704418

[10] Kim M, Jeong J, Lu H Z, et al. Conformal quantum dot–SnO_2 layers as electron transporters for efficient perovskite solar cells. Science, 2022, 375, 302

[11] Liu C, Sun J, Tan W L, et al. Alkali cation doping for improving the structural stability of 2D perovskite in 3D/2D PSCs. Nano Lett, 2020, 20, 1240

[12] Xie F X, Chen C C, Wu Y Z, et al. Vertical recrystallization for highly efficient and stable formamidinium-based inverted-structure perovskite solar cells. Energy Environ Sci, 2017, 10, 1942

[13] Xiang W C, Wang Z W, Kubicki D J, et al. Europium-doped $CsPbI_2Br$ for stable and highly efficient inorganic perovskite solar cells. Joule, 2019, 3, 205

[14] Yang S, Niu W X, Wang A L, et al. Ultrathin two-dimensional organic-inorganic hybrid perovskite nanosheets with bright, tunable photoluminescence and high stability. Angew Chem Int Ed, 2017, 56, 4252

[15] Sun Y, Yin Y, Pols M, et al. Engineering the phases and heterostructures of ultrathin hybrid perovskite nanosheets. Adv Mater, 2020, 32, 2002392

[16] Su Y, Chen X J, Ji W Y, et al. Highly controllable and efficient synthesis of mixed-halide $CsPbX_3$ (X = Cl, Br, I) perovskite QDs toward the tunability of entire visible light. ACS Appl Mater Interfaces, 2017, 9, 33020

[17] Utzat H, Sun W W, Kaplan A E K, et al. Coherent single-photon emission from colloidal lead halide perovskite quantum dots. Science, 2019, 363, 1068

[18] Filip M R, Hillman S, Haghighirad A A, et al. Band gaps of the lead-free halide double perovskites $Cs_2BiAgCl_6$ and $Cs_2BiAgBr_6$ from theory and experiment. J Phys Chem Lett, 2016, 7, 2579

[19] Zhong H X, Yang M, Tang G, et al. Type-II lateral heterostructures of monolayer halide double perovskites for optoelectronic applications. ACS Energy Lett, 2020, 5, 2275

[20] McClure E T, Ball M R, Windl W, et al. Cs_2AgBiX_6 (X = Br, Cl): New visible light absorbing, lead-free halide perovskite semiconductors. Chem Mater, 2016, 28, 1348

[21] Wu C C, Zhang Q H, Liu Y, et al. The dawn of lead-free perovskite solar cell: Highly stable double perovskite $Cs_2AgBiBr_6$ film. Adv Sci, 2018, 5, 1700759

[22] Volonakis G, Haghighirad A A, Milot R L, et al. $Cs_2InAgCl_6$: A new lead-free halide double perovskite with direct band gap. J Phys Chem Lett, 2017, 8, 772

[23] Li Z Z, Yin W J. Recent progress in Pb-free stable inorganic double halide perovskites. J Semicond, 2018, 39, 071003

[24] Xiao Z W, Yan Y F. Progress in theoretical study of metal halide perovskite solar cell materials. Adv Energy Mater, 2017, 7, 1701136

[25] Yang Y, Sun Y B, Jiang Y S. Structure and photocatalytic property of perovskite and perovskite-related compounds. Mater Chem Phys, 2006, 96, 234

[26] Zhang H, Fu X, Tang Y, et al. Phase segregation due to ion migration in all-inorganic mixed-halide perovskite nanocrystals. Nat Commun, 2019, 10, 1088

[27] Huang B Y, Liu Z H, Wu C W, et al. Polar or nonpolar? That is not the question for perovskite solar cells. Natl Sci Rev, 2021, 8, nwab094

[28] Lei Y T, Xu Y K, Wang M, et al. Origin, influence, and countermeasures of defects in perovskite solar cells. Small, 2021, 17, 2005495

[29] Wu J P, Liu S C, Li Z B, et al. Strain in perovskite solar cells: Origins, impacts and regulation. Natl Sci Rev, 2021, 8, nwab047

[30] Sin C K, Zhang J Z, Tse K, et al. A brief review of formation energies calculation of surfaces and edges in semiconductors. J Semicond, 2020, 41, 061101

[31] Bhattacharya S, Chandra G K, Predeep P. A microstructural analysis of 2D halide perovskites: Stability and functionality. Front Nanotechnol, 2021, 3, 657948

[32] Kim T W, Park N G. Methodologies for structural investigations of organic lead halide perovskites. Mater Today, 2020, 38, 67

[33] Kumar V, Nisika, Kumar M. Temporal-spatial-energy resolved advance multidimensional techniques to probe photovoltaic materials from atomistic viewpoint for next-generation energy solutions. Energy Environ Sci, 2021, 14, 4760

[34] Liu J J. Advances and applications of atomic-resolution scanning transmission electron microscopy. Microsc Microan, 2021, 27, 943

[35] Ribet S M, Murthy A A, Roth E W, et al. Making the most of your electrons: Challenges and opportunities in characterizing hybrid interfaces with STEM. Mater Today, 2021, 50, 100

[36] Zha F X, Zhang Q Y, Dai H G, et al. The scanning tunneling microscopy and spectroscopy of $GaSb_{1-x}Bi_x$ films of a few-nanometer thickness grown by molecular beam epitaxy. J Semicond, 2021, 42, 092101

[37] Yang Z, Liu S Z. Perspective on the imaging device based on perovskite materials. J Semicond, 2020, 41, 050401

[38] Rothmann M U, Li W, Zhu Y, et al. Direct observation of intrinsic twin domains in tetragonal $CH_3NH_3PbI_3$. Nat Commun, 2017, 8, 14547

[39] Zhang D L, Zhu Y H, Liu L M, et al. Atomic-resolution transmission electron microscopy of electron beam-sensitive crystalline materials. Science, 2018, 359, 675

[40] Zhu Y, Wang S, Li B, et al. Twist-to-untwist evolution and cation polarization behavior of hybrid halide perovskite nanoplatelets revealed by cryogenic transmission electron microscopy. J Phys Chem Lett, 2021, 12, 12187-95

[41] Yu Y, Zhang D D, Kisielowski C, et al. Atomic resolution imaging of halide perovskites. Nano Lett, 2016, 16, 7530

[42] Divitini G, Cacovich S, Matteocci F, et al. *In situ* observation of heat-induced degradation of perovskite solar cells. Nat Energy, 2016, 1, 15012

[43] Seo Y H, Kim J H, Kim D H, et al. *In situ* TEM observation of the heat-induced degradation of single- and triple-cation planar perovskite solar cells. Nano Energy, 2020, 77, 105164

[44] Ge Y, Mu X L, Lu Y, et al. Photoinduced degradation of lead halide perovskite thin films in air. Acta Phys Chim Sin, 2020, 36, 1905039

[45] Rothmann M U, Li W, Etheridge J, et al. Microstructural characterisations of perovskite solar cells - from grains to interfaces: Tech-

niques, features, and challenges. Adv Energy Mater, 2017, 7, 1700912
[46] Rothmann M U, Li W, Zhu Y, et al. Structural and chemical changes to $CH_3NH_3PbI_3$ induced by electron and gallium ion beams. Adv Mater, 2018, 30, 1800629
[47] Chen X Y, Wang Z W. Investigating chemical and structural instabilities of lead halide perovskite induced by electron beam irradiation. Micron, 2019, 116, 73
[48] Li Y B, Zhou W J, Li Y Z, et al. Unravelling degradation mechanisms and atomic structure of organic-inorganic halide perovskites by cryo-EM. Joule, 2019, 3, 2854
[49] Kim T W, Kondo T. Direction-selective electron beam damage to $CH_3NH_3PbI_3$ based on crystallographic anisotropy. Appl Phys Express, 2020, 13, 091001
[50] Alberti A, Bongiorno C, Smecca E, et al. Pb clustering and PbI_2 nanofragmentation during methylammonium lead iodide perovskite degradation. Nat Commun, 2019, 10, 2196
[51] Manekkathodi A, Marzouk A, Ponraj J, et al. Observation of structural phase transitions and PbI_2 formation during the degradation of triple-cation double-halide perovskites. ACS Appl Energy Mater, 2020, 3, 6302
[52] Dou L T, Wong A B, Yu Y, et al. Atomically thin two-dimensional organic-inorganic hybrid perovskites. Science, 2015, 349, 1518
[53] Nie L F, Ke X X, Sui M L. Microstructural study of two-dimensional organic-inorganic hybrid perovskite nanosheet degradation under illumination. Nanomaterials, 2019, 9, 722
[54] Li F, Liu Y, Wang H, et al. Postsynthetic surface trap removal of $CsPbX_3$ (X = Cl, Br, or I) quantum dots via a ZnX_2/hexane solution toward an enhanced luminescence quantum yield. Chem Mater, 2018, 30, 8546
[55] Su G D, He B L, Gong Z K, et al. Enhanced charge extraction in carbon-based all-inorganic $CsPbBr_3$ perovskite solar cells by dual-function interface engineering. Electrochim Acta, 2019, 328, 135102
[56] Dang Z Y, Shamsi J, Palazon F, et al. *In situ* transmission electron microscopy study of electron beam-induced transformations in colloidal cesium lead halide perovskite nanocrystals. ACS Nano, 2017, 11, 2124
[57] Zou S H, Liu C P, Li R F, et al. From nonluminescent to blue-emitting Cs_4PbBr_6 nanocrystals: Tailoring the insulator bandgap of 0D perovskite through Sn cation doping. Adv Mater, 2019, 31, 1900606
[58] Wang T, Yang Z, Yang L, et al. Atomic-scale insights into the dynamics of growth and degradation of all-inorganic perovskite nanocrystals. J Phys Chem Lett, 2020, 11, 4618
[59] Funk H, Shargaieva O, Eljarrat A, et al. *In situ* TEM monitoring of phase-segregation in inorganic mixed halide perovskite. J Phys Chem Lett, 2020, 11, 4945
[60] Zhou W, Han P, Zhang X, et al. Lead-free small-bandgap $Cs_2CuSbCl_6$ double perovskite nanocrystals. J Phys Chem Lett, 2020, 11, 6463
[61] Creutz S E, Crites E N, de Siena M C, et al. Colloidal nanocrystals of lead-free double-perovskite (elpasolite) semiconductors: Synthesis and anion exchange to access new materials. Nano Lett, 2018, 18, 1118
[62] Feng Y H, Ke X X, Sui M L. Effect of electron irradiation on inorganic double perovskite solar cell material $Cs_2AgBiBr_6$. J Chin Electron Microsc Soc, 2020, 39, 1
[63] Egerton R F, Li P, Malac M. Radiation damage in the TEM and SEM. Micron, 2004, 35, 399
[64] Gong Z L, Yang Y. The application of synchrotron X-ray techniques to the study of rechargeable batteries. J Energy Chem, 2018, 27, 1566
[65] Cai Z H, Wu Y N, Chen S Y. Energy-dependent knock-on damage of organic-inorganic hybrid perovskites under electron beam irradiation: First-principles insights. Appl Phys Lett, 2021, 119, 123901
[66] Chen Z X, Ke X X, Zhu L J, et al. Electron microscopy of organic-inorganic hybrid perovskite solar cell materials: degradation mechanism study and imaging condition optimization. J Chin Electron Microsc Soc, 2019, 38, 15
[67] Rothmann M U, Kim J S, Borchert J, et al. Atomic-scale microstructure of metal halide perovskite. Science, 2020, 370, 6516
[68] Chen S, Zhang X, Zhao J, et al. Atomic scale insights into structure instability and decomposition pathway of methylammonium lead iodide perovskite. Nat Commun, 2018, 9, 4807
[69] Chen S L, Zhang Y, Zhang X W, et al. General decomposition pathway of organic-inorganic hybrid perovskites through an intermediate superstructure and its suppression mechanism. Adv Mater, 2020, 32, 2001107
[70] Chen S L, Gao P. Challenges, myths, and opportunities of electron microscopy on halide perovskites. J Appl Phys, 2020, 128, 010901
[71] Chen S L, Zhang Y, Zhao J J, et al. Transmission electron microscopy of organic-inorganic hybrid perovskites: Myths and truths. Sci Bull, 2020, 65, 1643
[72] Zhou X G, Yang C Q, Sang X, et al. Probing the electron beam-induced structural evolution of halide perovskite thin films by scanning transmission electron microscopy. J Phys Chem C, 2021, 125, 10786
[73] Yuan B, Shi E Z, Liang C, et al. Structural damage of two-dimensional organic–inorganic halide perovskites. Inorganics, 2020, 8, 13
[74] Li W, Rothmann M U, Zhu Y, et al. The critical role of composition-dependent intragrain planar defects in the performance of $MA_{1-x}FA_xPbI_3$ perovskite solar cells. Nat Energy, 2021, 6, 624
[75] Gao Y, Shi E, Deng S, et al. Molecular engineering of organic–inorganic hybrid perovskites quantum wells. Nat Chem, 2019, 11, 1151
[76] Pan W, Wu H, Luo J, et al. $Cs_2AgBiBr_6$ single-crystal X-ray detectors with a low detection limit. Nat Photonics, 2017, 11, 726
[77] Luo J, Wang X, Li S, et al. Efficient and stable emission of warm-white light from lead-free halide double perovskites. Nature, 2018, 563, 541
[78] Pham H T, Yin Y T, Andersson G, et al. Unraveling the influence of CsCl/MACl on the formation of nanotwins, stacking faults and cubic supercell structure in FA-based perovskite solar cells. Nano Energy, 2021, 87, 106226
[79] Doherty T A S, Nagane S, Kubicki D J, et al. Stabilized tilted-octahedra halide perovskites inhibit local formation of performance-limiting phases. Science, 2021, 374, 1598
[80] Brennan M C, Kuno M, Rouvimov S. Crystal structure of individual $CsPbBr_3$ perovskite nanocubes. Inorg Chem, 2019, 58, 1555
[81] Song K P, Liu L M, Zhang D L, et al. Atomic-resolution imaging of halide perovskites using electron microscopy. Adv Energy Mater, 2020, 10, 1904006
[82] Chen S, Wu C, Han B, et al. Atomic-scale imaging of $CH_3NH_3PbI_3$ structure and its decomposition pathway. Nat Commun, 2021, 12, 5516
[83] Qiao G Y, Guan D H, Yuan S, et al. Perovskite quantum dots encapsulated in a mesoporous metal-organic framework as synergistic photocathode materials. J Am Chem Soc, 2021, 143, 14253
[84] dos Reis R, Yang H, Ophus C, et al. Determination of the structural phase and octahedral rotation angle in halide perovskites. Appl Phys Lett, 2018, 112, 071901
[85] VandenBussche E J, Clark C P, Holmes R J, et al. Mitigating damage to hybrid perovskites using pulsed-beam TEM. ACS Omega, 2020, 5, 31867
[86] Cai S H, Dai J, Shao Z P, et al. Atomically resolved electrically active intragrain interfaces in perovskite semiconductors. J Am Chem Soc, 2022, 144, 1910
[87] Shi E, Yuan B, Shiring S B, et al. Two-dimensional halide per-

ovskite lateral epitaxial heterostructures. Nature, 2020, 580, 614
[88] Jung H J, Stompus C C, Kanatzidis M G, et al. Self-passivation of 2D ruddlesden–popper perovskite by polytypic surface PbI_2 encapsulation. Nano Lett, 2019, 19, 6109
[89] Yu Y, Zhang D D, Yang P D. Ruddlesden-popper phase in two-dimensional inorganic halide perovskites: A plausible model and the supporting observations. Nano Lett, 2017, 17, 5489
[90] Dang Z Y, Dhanabalan B, Castelli A, et al. Temperature-driven transformation of $CsPbBr_3$ nanoplatelets into mosaic nanotiles in solution through self-assembly. Nano Lett, 2020, 20, 1808
[91] Kosasih F U, Cacovich S, Divitini G, et al. Nanometric chemical analysis of beam-sensitive materials: A case study of STEM-EDX on perovskite solar cells. Small Methods, 2021, 5, 2000835
[92] Liu J, Song K, Zheng X, et al. Cyanamide passivation enables robust elemental imaging of metal halide perovskites at atomic resolution. J Phys Chem Lett, 2021, 12, 10402
[93] Brescia R, Toso S, Ramasse Q, et al. Bandgap determination from individual orthorhombic thin cesium lead bromide nanosheets by electron energy-loss spectroscopy. Nanoscale Horiz, 2020, 5, 1610
[94] Li Y B, Huang W, Li Y Z, et al. Opportunities for cryogenic electron microscopy in materials science and nanoscience. ACS Nano, 2020, 14, 9263
[95] Zhang Z W, Cui Y, Vila R, et al. Cryogenic electron microscopy for energy materials. Acc Chem Res, 2021, 54, 3505
[96] Zhu Y M, Gui Z G, Wang Q, et al. Direct atomic scale characterization of the surface structure and planar defects in the organic-inorganic hybrid $CH_3NH_3PbI_3$ by Cryo-TEM. Nano Energy, 2020, 73, 104820
[97] Zhu Y M, Zhang Q, Yang X M, et al. Probing atomic structure of beam-sensitive energy materials in their native states using cryogenic transmission electron microscopes. iScience, 2021, 24, 103385
[98] Dang Z Y, Shamsi J, Akkerman Q A, et al. Low-temperature electron beam-induced transformations of cesium lead halide perovskite nanocrystals. ACS Omega, 2017, 2, 5660
[99] Rivas N A, Babayigit A, Conings B, et al. Cryo-focused ion beam preparation of perovskite based solar cells for atom probe tomography. PLoS One, 2020, 15, e0227920
[100] Zhou J F, Wei N N, Zhang D L, et al. Cryogenic focused ion beam enables atomic-resolution imaging of local structures in highly sensitive bulk crystals and devices. J Am Chem Soc, 2022, 144, 3182
[101] Lee J W, Seo S, Nandi P, et al. Dynamic structural property of organic-inorganic metal halide perovskite. iScience, 2021, 24, 101959
[102] Stranks S D. Multimodal microscopy characterization of halide perovskite semiconductors: Revealing a new world (dis)order. Matter, 2021, 4, 3852
[103] Thampy S, Xu W J, Hsu J W P. Metal oxide-induced instability and its mitigation in halide perovskite solar cells. J Phys Chem Lett, 2021, 12, 8495
[104] Zhang C C, Yuan S, Lou Y H, et al. Physical fields manipulation for high-performance perovskite photovoltaics. Small, 2022, 2107556
[105] Kosasih F U, Ducati C. Characterising degradation of perovskite solar cells through *in situ* and operando electron microscopy. Nano Energy, 2018, 47, 243
[106] Kundu S, Kelly T L. *In situ* studies of the degradation mechanisms of perovskite solar cells. EcoMat, 2020, 2, e12025
[107] McGrath F, Ghorpade U V, Ryan K M. Synthesis and dimensional control of $CsPbBr_3$ perovskite nanocrystals using phosphorous based ligands. J Chem Phys, 2020, 152, 174702
[108] Jeangros Q, Duchamp M, Werner J, et al. *In situ* TEM analysis of organic-inorganic metal-halide perovskite solar cells under electrical bias. Nano Lett, 2016, 16, 7013
[109] Jung H J, Kim D, Kim S, et al. Stability of halide perovskite solar cell devices: *in situ* observation of oxygen diffusion under biasing. Adv Mater, 2018, 30, 1802769
[110] Kim M C, Ahn N, Cheng D Y, et al. Imaging real-time amorphization of hybrid perovskite solar cells under electrical biasing. ACS Energy Lett, 2021, 6, 3530
[111] Zhang C, Fernando J F S, Firestein K L, et al. Crystallography-derived optoelectronic and photovoltaic properties of $CsPbBr_3$ perovskite single crystals as revealed by *in situ* transmission electron microscopy. Appl Mater Today, 2020, 20, 100788
[112] Akhavan Kazemi M A, Raval P, Cherednichekno K, et al. Molecular-level insight into correlation between surface defects and stability of methylammonium lead halide perovskite under controlled humidity. Small Methods, 2021, 5, 2000834
[113] Qin F Y, Wang Z W, Wang Z L. Anomalous growth and coalescence dynamics of hybrid perovskite nanoparticles observed by liquid-cell transmission electron microscopy. ACS Nano, 2016, 10, 9787

Xiaomei Wu got her BS and master's degrees in 2018 and 2021 at Beijing Technology and Business University. Now she is a doctoral student at Beijing University of Technology. Her research focuses on energy materials microstructure characterization using TEM.

Xiaoxing Ke is an associate professor at Beijing University of Technology (BJUT), China. She received her Ph.D. degree from Physics Department, University of Antwerp, Belgium in 2010. After 4 years of postdoctoral fellowship in EMAT, University of Antwerp, she joined BJUT in 2014. Her research interests mainly focus on microstructure investigation on energy materials using advanced transmission electron microscopy (TEM), including aberration-corrected (S)TEM and 3D electron tomography.

Manling Sui is a Distinguished Professor at Beijing University of Technology (BJUT). She received her Ph.D. in 1991 at Institute of Metal Research, Chinese Academy of Sciences, and successively worked at Northeastern University in China, University of Wisconsin-Madison in the United States, and Institute of Metal Research, Chinese Academy of Sciences. Then she joined BJUT as Distinguished Professor of Cheung Kong Scholars Programme in 2009. Her research is focused on the structure and property relationships of advanced materials at atomic scale, especially using in situ transmission electron microscopy with external stimuli such as thermal, electrical, mechanical, optical, and liquid/gas environments.